Environment International 168 (2022) 107460

Contents lists available at ScienceDirect

Environment International

journal homepage: www.elsevier.com/locate/envint

Full length article

Mechanism insights into bacterial sporulation at natural sphalerite interface with and without light irradiation: The suppressing role in bacterial sporulation by photocatalysis

Wanjun Wang, Yan Liu, Guiying Li, Zhenni Liu, Po Keung Wong, Taicheng An *

Guangdong Key Laboratory of Environmental Catalysis and Health Risk Control, Guangdong-Hong Kong-Macao Joint Laboratory for Contaminants Exposure and Health, Institute of Environmental Health and Pollution control, Guangdong University of Technology, Guangzhou 510006, China
Guangzhou Key Laboratory of Environmental Catalysis and Pollution Control, Guangdong Engineering Technology Research Center for Photocatalytic Technology Integration and Equipment, School of Environmental Science and Engineering, Guangdong University of Technology, Guangzhou 510006, China

ARTICLE INFO

Handling Editor: Adrian Covaci

Keywords:
Bacterial sporulation
Natural sphalerite
Photocatalysis
Sporulation mechanism
Physiological response

ABSTRACT

Unveiling the mechanisms of bacterial sporulation at natural mineral interfaces is crucial to fully understand the interactions of mineral with microorganism in aquatic environment. In this study, the bacterial sporulation mechanisms of *Bacillus subtilis* (*B. subtilis*) at natural sphalerite (NS) interface with and without light irradiation were systematically investigated for the first time. Under dark condition, NS was found to inactivate vegetative cells of *B. subtilis* and promote their sporulation simultaneously. The released Zn^{2+} from NS was mainly responsible for the bacterial inactivation and sporulation. With light irradiation, the photocatalytic effect from NS could increase the bacterial inactivation efficiency, while the bacterial sporulation efficiency was decreased from 8.1 % to 4.5 %. The photo-generated H_2O_2 and $^{\bullet}O_2^-$ played the major roles in enhancing bacterial inactivation and suppressing bacterial sporulation process. The intracellular synthesis of dipicolinic acid (DPA) as biomarker for sporulation was promoted by NS in dark, which was suppressed by the photocatalytic effect of NS with light irradiation. The transformation process from vegetative cells to spores was monitored by both 3D-fluerecence EEM and SEM observations. Compared with the NS alone system, the NS/light combined system induced higher level of intracellular ROSs, up-regulated antioxidant enzyme activity and decreased cell metabolism activity, which eventually led to enhanced inactivation of vegetative cells and suppressed bacterial sporulation. These results not only provide in-depth understanding about bacterial sporulation as a new mode of sub-lethal stress response at NS interface, but also shed lights on putting forward suitable strategies for controlling spore-producing bacteria by suppressing their sporulation during water disinfection.

1. Introduction

Microorganisms and minerals are ubiquitous in nature, inevitably have physicochemical interactions in water environments (Lu et al., 2012), and play a pivotal role in water ecosystems. Minerals not only provide nutrients to microorganisms, but also play a role in inhibiting or promoting microbial growth (McMahon et al., 2016; Wilson and Butterfield, 2014). In return, microbes can influence mineral composition through biomineralization, crystallization, decomposition and weathering via microbial metabolism activities (Zhou et al., 2016). The interaction of minerals with microorganisms has attracted the interest of many scientists over the past few decades, and the applications and impacts have expanded significantly (Cuadros, 2017; Mueller, 2015). For example, microorganisms can capture K^+ from the environment and provide K^+ for bacterial mineralization via metabolic activities (Aubineau et al., 2019). Also, it has been discovered recently that natural sphalerite nanoparticles can promote plasmid-mediated horizontal transfer of drug resistance genes (Li et al., 2020). However, most of the existing works have only focused on the interactions of minerals with normal vegetative bacteria. In natural environment, a large portion of microorganisms are spore-producing bacteria, which may produce dominant spores when they encountering adverse environmental conditions.

Bacterial spores are known to be the most tenacious form of

* Corresponding author at: Guangdong Key Laboratory of Environmental Catalysis and Health Risk Control, Guangdong-Hong Kong-Macao Joint Laboratory for Contaminants Exposure and Health, Institute of Environmental Health and Pollution control, Guangdong University of Technology, Guangzhou 510006, China.
E-mail address: antc99@gdut.edu.cn (T. An).

https://doi.org/10.1016/j.envint.2022.107460
Received 1 June 2022; Received in revised form 22 July 2022; Accepted 7 August 2022
Available online 10 August 2022

microorganisms, which are extremely resistant to unfavorable environments and are resistant to heat, alkali, acid, hypertonicity and radiations. Once the dominant spores are exposed to a more advantageous environment, they can be re-activated and pose greater threats to human health (De Sordi et al., 2015; Li et al., 2018a). For example, *Bacillus cereus* spores could be germinated and produce toxins that may cause abdominal pain, diarrhea, and nausea (Tewari and Abdullah, 2015). Therefore, understanding the interaction mechanisms between natural minerals and spore-producing bacteria in aquatic environment is crucial to fully reveal the mineral/microorganism interaction mechanisms, which can also provide guidance for developing novel strategies to control bacterial spore-contaminated water pollution.

Various environmental factors have been reported to be able to stimulate vegetative cells of *Bacillus* sp. to produce spores, including temperature, pH, dissolved oxygen and metal elements (e.g. Mn(II), Ca (II), etc.) (Mtimet et al., 2015; Sella et al., 2014). For instance, Sinnelä et al. (2019) has found that a certain concentration ratio of Ca^{2+} and Mn^{2+} can promote the sporulation of *Bacillus* sp., and a large amount of dipicolinic acid (DPA) complex is synthesized by chelating with Ca^{2+} (Nishikawa and Kobayashi, 2021). Natural minerals can also significantly deform bacterial cells of *E. coli* by disrupting and stiffening flagella (Zhang et al., 2012), inhibiting DNA replication (Li et al., 2013), or inducing DNA breaks (González-Tortuero et al., 2018). However, the most widely investigated *E. coli* cannot produce spores. Whether the natural minerals could stimulate vegetative cells of spore-producing bacteria to form spores and the sporulation mechanisms remains a mystery. In addition, natural minerals always co-exist with light irradiation in many environmental systems. If the natural mineral nanoparticle has suitable semiconductor band structure characterized by an electron fully occupied valence band (VB) and an empty conduction band (CB), a photocatalytic interface can be constructed by combing minerals with light irradiation. In this case, photo-generated electron (e^-) – hole (h^+) pairs will be produced after absorbing photons and then generate reactive oxygen species (ROSs) (e.g. $^{\bullet}OH$, $^{\bullet}O_2^-$, $^1O_2$, H_2O_2, etc.) after a series of reactions (Li et al., 2015; Qi et al., 2022; Wang et al., 2020). These ROSs generated in photocatalytic processes have strong oxidation power, which are widely used in environmental remediation including organic pollutant degradation and bacterial inactivation (Liu et al., 2021; Liu et al., 2022; Wang et al., 2017). Chen et al. (2011) was the first report to use natural sphalerite as photocatalysts for bacterial inactivation. Following this work, natural magnetic sphalerite, natural pyrite and natural hematite-alginate have also been employed to be capable of inactivating *E. coli* cells (Mohammadi et al., 2021; Moradi et al., 2017; Peng et al., 2017). However, besides the lethal inactivation, when the oxidative stress mediated by ROSs is not high enough to cause completely lethal inactivation, the cells would also enter into sub-lethal states by forming biofilm, viable but nonculturable bacterial cell (VBNC) states, inducing sporulation, etc (Cai et al., 2021). For instance, the growth of biofilm could be inhibited by sub-lethal photocatalysis with the decrease of bacterial number in VBNC states (Chen et al., 2022). The sub-lethal stress response under light irradiation and photocatalytic treatment could promote the conjugate transfer frequency of antibiotic resistance genes (Chen et al., 2019; Yin et al., 2021). However, all these existing studies only focused on vegetative cells that could not produce spores (*i.e.*, *E. coli*), but did not explore the cells which can produce spores to alleviate oxidative stress. Bacterial sporulation, as an important and long-existed mode of sub-lethal stress response has not received adequate investigation. Although there were few studies that reported the inactivation of bacterial spores by using artificially synthesized photocatalytic nanoparticles (e.g. N/C-doped TiO_2, Ag/Pt-doped TiO_2), the photocatalyst synthesis and inactivation efficiency of nanoparticles were their research focus (Berberidou et al., 2012; Chen et al., 2021). The biological stress response during the transformation from vegetative cells to bacterial spores with and without light stimulation has not been investigated yet.

In this work, bacterial sporulation performances and formation mechanisms at the natural mineral interfaces were systematically studied in the absence/presence of light irradiation, using natural sphalerite (NS) and *Bacillus subtilis* (*B. subtilis*) as model mineral and bacteria, respectively. The bacterial inactivation and sporulation efficiency were simultaneously monitored, and sporulation mechanisms in terms of antioxidant enzyme activity, DPA synthesis and release, as well as cell morphology changes were also investigated. The objectives of this study were: (1) to clarify whether NS, light irradiation alone and NS/light combined treatment could promote or inhibit bacterial sporulation; (2) to identify the roles of different ROSs in determining the bacterial inactivation and sporulation efficiency; and (3) to reveal the different physiological stress response during bacterial sporulation in light, NS alone and NS/light combined systems. To the best of our knowledge, this is the first study focusing on the bacterial sporulation as a new mode of sub-lethal stress response at the interface of photocatalytic natural minerals, which could also provide in-depth insights into the interacting mechanisms of natural minerals with spore-producing bacteria and understand the photocatalytic effect on the evolution mechanism of spore-producing bacteria in aquatic environment.

2. Experimental section

2.1. Characterization of NS minerals

The NS used in the study was collected from ore deposit of Huangshaping in Hunan Province, China. The original NS was mechanically crushed, and sieved through 340-mesh to obtain fine powders according to previous study (Li et al., 2020, Yin et al., 2021). The obtained NS was characterized by X-ray diffraction (XRD) (Rigaku, Japan, Cu Kα, λ = 0.15406), and results indicated the main component was zinc sulfide (ZnS) (Fig. S1). Scanning electron microscopy (SEM) (TESCAN, MIRA LMS) equipped with Energy dispersive spectroscopy (EDS) were used to characterize the morphology and element distribution. The NS minerals exhibited irregular particles with sizes<30 μm, and EDS mapping images confirmed that the main component was ZnS (>80 % wt) with doping of impurity levels including Fe, Ca, Mg and Mn (Fig. S2). Pure ZnS powders (Sigma, 99.99 %) were also used as reference samples for the comparison. The NS suspension was prepared with ultrapure water (Millipore, Molsheim France) and the suspension was sterilized before use. The metal ion release in the NS suspension was monitored by using Inductively Coupled Plasma Mass Spectrometry (ICP-MS) (ICAP RQ, Thermo Fisher, Germany).

2.2. Bacterial sporulation experiments

B. subtilis ATCC6633 (Qingdao Hope Biotechnology, China) was used as a model spore-producing bacterial strain, since it was one of the most widely investigated spore-producing bacteria. Single colony of *B. subtilis* was inoculated in Nutrient Broth (Oxoid, UK) and incubated at 37 °C for 16 h to reach stationary phase. The cell density could be maintained at a constant value in the stationary phase. The optical density (OD_{600}) measured by Microplate Reader (Varioskan LUX; Thermo Fisher Scientific, USA) was approximately 1.0, corresponding to the cell density of $\sim 1.0 \times 10^9$ colony forming units (cfu)/mL. About 50 mL of the bacterial culture in Nutrient Broth was transferred in 250 mL conical flask with NS concentrations of 0–2.0 g/L. The flasks were then put into an incubator (Shanghai Yiheng, China) equipped with a fluorescent tubes as light source and incubated at 37 °C for 48 h to induce sporulation with and without light irradiation. In the case of light irradiation, the light intensity was adjusted to 2.5 mW/cm^2, measured by a light meter (PLS-MW 2000, Perfect Light, China). At given time intervals, aliquots of the bacterial culture were collected, serial diluted and spread on NB agar (Oxoid, UK) to determine the total number of viable cells (vegetative cells + spores) after incubated at 37 °C for 20 h.

The bacterial spore density was determined after high-temperature removal of vegetative cells according to the reported literatures

(Pandey et al., 2013). Briefly, aliquots of the bacterial culture were first heated at 80 °C for 20 min to remove all the vegetative cells. Then, the obtained spore culture was heated at 70 °C for 10 min to induce spore germination. Finally, the germinated spore aliquots were spread on NB agar (Oxoid, UK) incubated at 37 °C for 20 h to determine the spore density. The sporulation efficiency was calculated by the following Equation (1):

$$\text{Sporulation efficiency}\,(\%) = C_{(SP)t}/C_0 \times 100 \quad (1)$$

where $C_{(SP)t}$ represents the spore density at treatment time (t) and C_0 represents the total viable cell density at initial time (0).

The relative percentages of inactivated vegetative cells (IVC), produced spores (SP) and un-inactivated vegetative cells (UIVC) were determined by the following Equations (2) - (4):

$$\text{IVC}\,(\%) = (C_0 - C_{(total)t})/C_0 \times 100 \quad (2)$$

$$\text{SP}\,(\%) = C_{(SP)t}/C_0 \times 100 \quad (3)$$

$$\text{UIVC}\,(\%) = 100 - \text{IVC}(\%) - \text{SP}(\%) \quad (4)$$

where C_0 represents the total viable cell density at initial time (0), $C_{(total)t}$ is the total remaining cell density at treatment time (t), and $C_{(SP)t}$ represents the produced spore density at treatment time (t).

To evaluate the effects of different ROSs on the bacterial inactivation and sporulation, scavenger studies were performed by adding isopropanol (0.5 mmol/L), 4-hydroxy-2,2,6-tetramethylpiperidine oxygen (TEMPOL) (2 mmol/L) and catalase (300 U/mL) as $^{\bullet}OH$, $^{\bullet}O_2^-$ and H_2O_2 scavenger, respectively (Sheng et al., 2014; Wang et al., 2021; Zhang et al., 2010). All the experiments were conducted in triplicates, and the data were presented as the mean ± the standard deviation (SD). A one-way analysis of variation (ANOVA) was performed to determine the statistical difference of sporulation efficiency in NS alone and NS/light combined system. $P < 0.05$ indicated the difference was significant at the 95 % confidence interval.

2.3. Analytical methods

2.3.1. Detection of free radicals

The generation of free radicals (i.e. $^{\bullet}OH$ and $^{\bullet}O_2^-$) was verified by Electron Paramagnetic Resonance (EPR) technology. EPR signals of spin-trapped paramagnetic species with 5,5-dimethyl-1-pyrroline *N*-oxide (DMPO) were recorded with a Bruker EMXPlus EPR spectrometer. Typically, 100 mM of DMPO was added to a methanol ($^{\bullet}O_2^-$) or aqueous ($^{\bullet}OH$) dispersion of NS (0.1 g/L), and the EPR signals were collected in-situ during the light irradiation.

2.3.2. Dipicolinic acid (DPA) synthesis and release

To determine the intracellular DPA synthesis and distinguish vegetative cells/spores, three-dimensional fluorescence Excitation-Emission-Matrix (EEM) spectra of cell suspensions were measured with excitation wavelength of 300–600 nm and emission wavelength of 300–800 nm using a fluorescence spectrometer (FLS1000, Edinburgh, UK) according to (Smith et al., 2004). The quantification of DPA release was conducted by adding $TbCl_3$ to form DPA-Tb complex, following by quantified using fluorescence method (Kort et al., 2005). Briefly, 100 μL of the cell suspension was transferred to 96-well microtiter plate with 100 μL $TbCl_3$ (20 μM) in sodium acetate buffer (pH 5.0). After mixing for 15 min, the mixture was measured with excitation wavelength of 270 nm and emission wavelength of 545 nm in a microtiter plate fluorometer (Varioskan LUX, Thermo Fisher Scientific, USA) (Li et al., 2018b).

2.3.3. Cell morphology and membrane integrity

Scanning electron microscopy (SEM, Quanta 250 FEG, FEI, USA) was used to characterize the morphology of bacteria and spores. The detailed SEM sample preparation protocol was outlined in the SI. A modified Wirtz-Conklin staining was used to distinguish vegetative cells and spores (Hamouda et al., 2002). Briefly, cell suspensions were stained with malachite green, counterstained with safranine, and then observed by an optical microscopy (CX33, OLYMPUS, Japan). The cell membrane integrity was determined using SYTO 9/PI fluorescence assay (Fan et al., 2019). Samples of bacterial suspension were stained with SYTO 9 and PI in dark for 15 min, and 2 μL of bacterial solution was spread on a slide and observed under a fluorescent microscopy (DM6B, Leica Microsystems ltd, Germany).

2.3.4. Physiological responses of cells

To investigate the physiological responses of cells during sporulation, ATP synthesis ability was evaluated using an enhanced ATP detection kit (S0027, Beyotime). Intracellular ROSs levels were detected using the fluorescent dye 2′,7′-dichlorofluorescein diacetate (DCFH-DA) with Reactive Oxygen Species Detection Kit (S0033, Boyotime). Intracellular proteins were extracted using Bacterial Protein Extraction Kit (C600596, Biotech) and quantified by Modified Bradford Protein Assay Kit (C503041, Biotech). Catalase (CAT) activity was determined by a Peroxidase Assay Kit (S0051, Boyotime) following the manufacturer's instructions.

3. Results and discussion

3.1. Bacterial sporulation at the interface of NS mineral in dark

To investigate the interactions between NS and *B. subtilis* cells, the bacterial sporulation experiments were first conducted in dark conditions. Fig. 1a shows the changes of total viable cell density of *B. subtilis* co-cultured with different concentrations of NS mineral. In the control experiments, ~1.0 log of viable cells was inactivated after culturing for 48 h, due to nutrient depletion causing cells to die naturally. When the *B. subtilis* cells were co-cultured with NS mineral, enhanced inactivation efficiency was observed and ~ 2.2 log reduction of viable cells was found within 48 h in the presence of 0.1 g/L NS mineral. When further increasing the NS concentration from 0.1 to 2.0 g/L, the bacterial inactivation efficiency was increased proportionally, and ~ 5.5 log reduction of viable cells was achieved with 2.0 g/L NS. The *B. subtilis* sporulation efficiency was simultaneously monitored as shown in Fig. 1 (b). In the control experiments, very limited *B. subtilis* spores with sporulation efficiency of only 0.2 % were found after cultivation for 48 h. In contrast, the sporulation efficiency was increased dramatically to 7.83 % in the presence of 0.1 g/L NS mineral, suggesting the mineral could indeed stimulate the vegetative cells of *B. subtilis* to produce spores. However, with the increase of NS concentration from 0.1 to 2.0 g/L, the sporulation efficiency was gradually decreased from 7.83 % to 0.11 %. These results indicated that high concentration of NS could result in high lethal effect on *B. subtilis* cells, while a moderate concentration of NS might cause sub-lethal effect which could stimulate the cells to transform to spores. It was further found that when decreasing the NS concentration from 0.1 to 0.02 g/L, the sporulation efficiency was decreased from 7.83 % to 0.12 % (Fig. S3). Therefore, a clear dose–effect relationship was found between NS concentration and bacterial inactivation/sporulation efficiency. Specifically, 0.1 g/L NS exhibited the optimal sub-lethal effect which could produce the highest numbers of spores. Thus, in order to study the sporulation mechanisms and subsequent inhibition effects by light irradiation, 0.1 g/L NS mineral which can achieve the highest sporulation efficiency was used in the subsequent experiments.

It was found that 5.5 mg/L Zn^{2+} and trace amounts of Ca^{2+}, Fe^{2+}, Mg^{2+}, Mn^{2+} were released in 0.1 g/L NS mineral suspension (Fig. S4). Therefore, equivalent amounts of Zn^{2+} (5.5 mg/L) and pure ZnS nanoparticles (0.1 g/L) were used as reference samples to compare the bacterial inactivation and sporulation efficiency with the NS mineral (0.1 g/L) (Fig. S5). Almost no bacterial inactivation was found with pure ZnS, while ~ 2.2 log of viable cells was inactivated by Zn^{2+}, and the efficiency was similar to that of NS mineral. The high toxicity of Zn^{2+} for

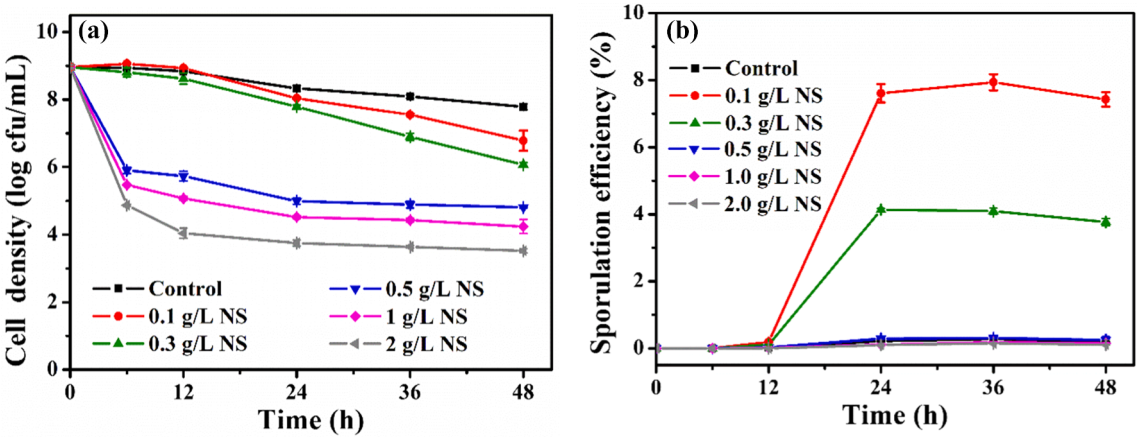

Fig. 1. (a) Changes of viable cell density and (b) sporulation efficiency of *B. subtilis* at NS interface under dark condition. Experimental condition: [Cell] = 1.0×10^9 cfu/mL, [NS] = 0.1–2.0 g/L, $[pH]_0$ = 8.5.

bacterial inactivation was also evidenced in previous studies (Singh et al., 2019, Xu et al., 2016). These results indicated that under dark condition, the released Zn^{2+} from NS was the main reason to cause bacterial inactivation, which also imposed sub-lethal effective to stimulate bacterial sporulation as shown in Fig. 1b.

3.2. Bacterial sporulation at the interface of NS mineral with light irradiation

To study the light irradiation effect on *B. subtilis* sporulation at the NS interface, the experiments were then conducted under irradiation of fluorescent tube to simulate sunlight irradiation. Fig. 2a compares the bacterial inactivation efficiency of *B. subtilis* in the control, light irradiation, NS alone and NS/light combined system. The light treatment

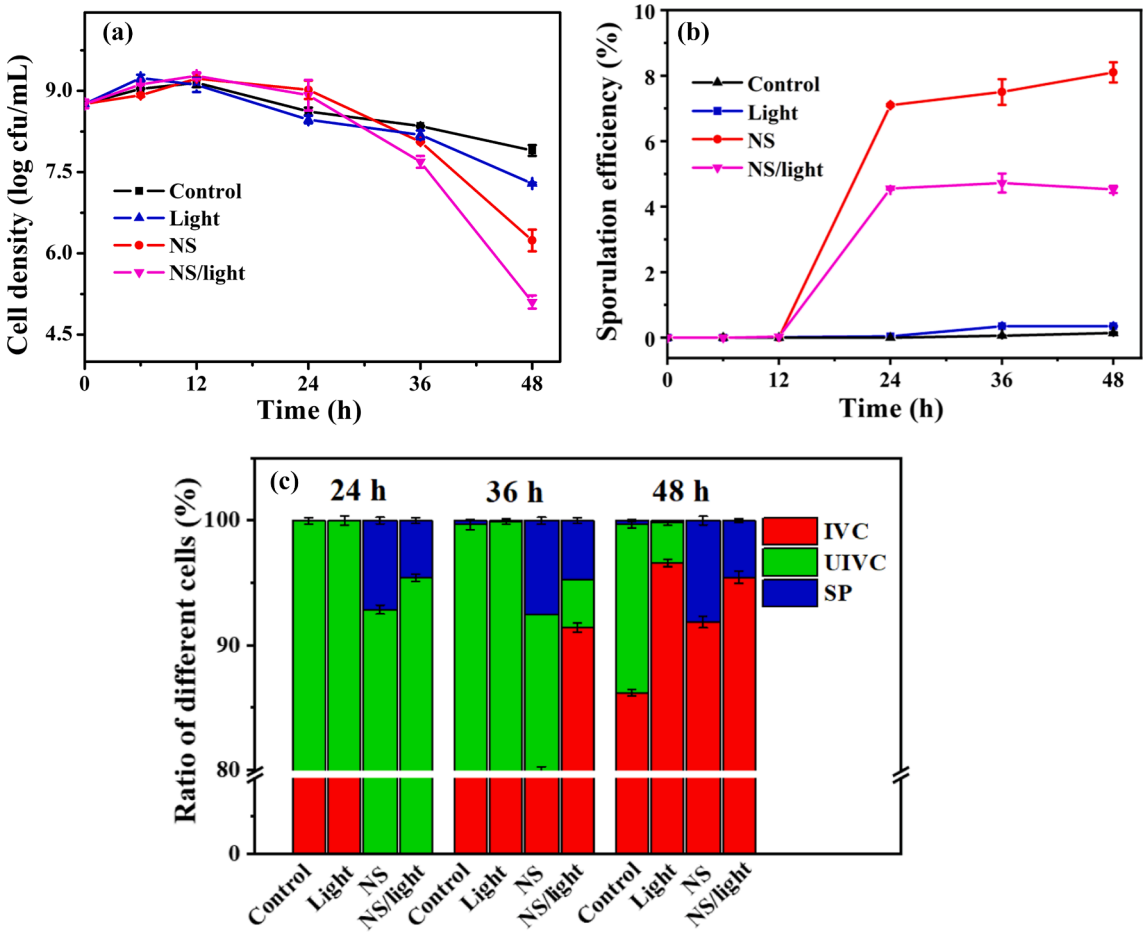

Fig. 2. (a) Changes of viable cell density, (b) sporulation efficiency and (c) ratios of different statues of *B. subtilis* cells at NS interface together with light irradiation (IVC: inactivated vegetative cells; UIVC: un-inactivated vegetative cells; SP: produced spores). Experimental condition: [Cell] = 1.0×10^9 cfu/mL, [NS] = 0.1 g/L, $[pH]_0$ = 8.5.

could inactivate ~ 1.5 log of viable cells within 48 h, with inactivation efficiency higher than that of the control groups, suggesting light alone could inactivate the *B. subtilis* cells to some extent. This might be due to the trace amounts of UV light emitted from the fluorescent tube, which could slightly inactivate the bacterial cells. The NS alone system showed enhanced bacterial inactivation efficiency than that of light system. Notably, the NS/light combined system exhibited the highest bacterial inactivation efficiency, and ~ 3.5 log of viable cells could be inactivated within 48 h. This indicated the photocatalytic effect at NS interface could effectively promote the inactivation of the *B. subtilis* cells, which was similar to previous report about *E. coli* inactivation (Chen et al., 2011). The inactivation kinetics was studied according to the log-linear-shoulder model proposed by (Geeraerd et al., 2005; Wang et al., 2019) (Equation (5)):

$$N_t = (N_0 - N_{res}) * e^{-k_{max} t} * \left(\frac{e^{k_{max} S_l}}{1 + (e^{k_{max} S_l} - 1) * e^{-k_{max} t}} \right) + N_{res} \quad (5)$$

where N_0 is the initial cell destiny (cfu/mL), N_{res} is the residual cell density (cfu/mL), k_{max} is inactivation rate constant (h^{-1}) and S_l is the shoulder length (h). The k_{max} was calculated to be 0.15, 0.36 and 0.50 h^{-1} for bacterial inactivation in light alone, NS alone and NS/light combined system, respectively (Table S1). At the initial stage (<24 h), the cell density remained almost constant due to the protection from the bacterial defending system. With the increase and accumulation of produced ROSs, the bacterial defending system was collapsed, leading to the dramatic increase of inactivation kinetics. Meanwhile, the sporulation efficiencies in control, light irradiation, NS alone and NS/light combined systems were compared (Fig. 2b). The control and light alone systems exhibited similar and low sporulation efficiency (<0.5 %), while the NS alone system showed significantly higher sporulation efficiency of 8.1 % within 48 h, indicating the NS alone could really promote bacterial sporulation. However, the sporulation efficiency in the NS/light combined system was decreased significantly to 4.5 % ($P < 0.05$) (Fig. S6). In addition, when the NS concentration was 0.08 g/L, the sporulation efficiency at the NS interface within 48 h was also decreased significantly from 4.43 % to 2.43 % after light irradiation ($P < 0.05$) (Fig. S7). These results suggested that the photocatalytic effect arisen from the NS mineral could effectively suppress the bacterial sporulation.

At the beginning, all the *B. subtilis* cells existed in vegetative form without spores. During co-cultivation with NS mineral, some of vegetative cells were inactivated while some of the cells transformed to spores. Therefore, the bacterial status in the cultivation system can be divided into three parts: the inactivated vegetative cells (IVC), the un-inactivated vegetative cells (UIVC) and the produced spores (SP). To further elucidate the variation of bacterial status, changes of the proportion of the three statuses were analyzed (Fig. 2c). In general, the proportion of IVC was increased with the decease of UIVC and occurrence of SP in the cultivation processes, suggesting the inactivation of vegetative cells was always accompanied with spore formation due to sub-lethal effect. In light alone system, the proportion of IVC was increased steadily to reach ~ 96.6 % with the appearance of ~ 3.2 % UIVC and ~ 0.2 % SP within 48 h. In the NS alone system, the proportion of IVC was 91.9 % with SP to be 8.1 %, and no UIVC was found, suggesting all *B. subtilis* cells was transformed to spores leaving no alive vegetative cells at the end of 48 h. However, in the NS/light combined system, the proportion of IVC was obtained as 95.5 %, which was higher than that in the NS alone system. The proportion of SP was lower than that in the NS alone system, and also no UIVC was found. These results indicated that more vegetative cells of *B. subtilis* was killed in the NS/light combined system before they could transform to spores, leading to the suppressed sporulation performances. In the NS/light combined system, the photocatalytic effect could produce various kinds of ROSs, which might be involved in the sporulation processes.

Thus, scavenging study was then conducted to investigate the roles of different photo-generated ROSs in the bacterial inactivation and sporulation process. In light alone and NS alone systems, the addition of scavengers would not influence the bacterial inactivation and sporulation efficiencies (Fig. S8), suggesting there were no external ROSs generated in the light and NS alone systems. In the NS/light combined system, Fig. 3a shows that the addition of isopropanol as $^{\bullet}OH$ scavenger has no influence on the bacterial inactivation efficiency, suggesting $^{\bullet}OH$ is not a major reactive species. When adding catalase (H_2O_2 scavenger) and TEMPOL ($^{\bullet}O_2^-$ scavenger), the bacterial inactivation was significantly inhibited, suggesting H_2O_2 and $^{\bullet}O_2^-$ might be the dominant ROSs, which was consistent with previous studies (Chen et al., 2011). In the sporulation processes, the addition of isopropanol also had negligible effect on the sporulation efficiency, while the addition of catalase and TEMPOL could significantly increase the sporulation efficiency (Fig. 3b). This result showed that the decreased bacterial inactivation by scavenging H_2O_2 and $^{\bullet}O_2^-$ could lead to the promoted spore formation, which in turn indicated that H_2O_2 and $^{\bullet}O_2^-$ were the major reactive species for suppressing bacterial sporulation. In addition, the radical generation was verified by EPR spectroscopy using DMPO as spin-trapping reagent. As shown in Fig. 3c, obvious peaks corresponding to the DMPO–$^{\bullet}O_2^-$ adducts were observed, while no signals for the DMPO–$^{\bullet}OH$ adducts were observed, further confirming the generation of $^{\bullet}O_2^-$ rather than $^{\bullet}OH$ radicals. The proportion of IVC, UIVC and SP was further displayed in Fig. 3d. It showed that the UIVC was decreased with the increase of IVC and SP, which was ascribed to the lethal and sub-lethal effect respectively. The proportion of SP when adding catalase and TEMPOL was 7.56 % and 6.93 %, which was higher than that of 4.5 % without scavengers. Therefore, it is assumed that if H_2O_2/$^{\bullet}O_2^-$ was removed in this system, sub-lethal effect would be pronounced thus leading to the enhanced sporulation efficiency, and vice versa. To confirm this hypothesis, experiments were conducted by external adding H_2O_2 in the NS alone system, and it was found the sporulation efficiency was decreased from ~ 8.1 % to ~ 5.7 % with external H_2O_2 addition (Fig. S9). These results doubly confirmed that H_2O_2/$^{\bullet}O_2^-$ was the major reactive species for bacterial inactivation, which could also suppress the bacterial sporulation efficiency.

3.3. Mechanisms of bacterial sporulation

3.3.1. Monitoring of DPA synthesis and release

DPA is a major constituent of bacterial spores (5–15 % of dry weight), which is involved in spore dormancy and germination. It is often used as a biomarker of bacterial spores (Redan et al., 2022; Tehri et al., 2018). DPA is synthesized in sporulating cells from dihydroxydipicolinic acid and chelated with divalent cations (e.g. Ca^{2+}, Mn^{2+}) or germination-specific lytic enzymes (GSLEs) to form the complex. The produced DPA complex show enhanced fluorescence with excitation wavelength of 320–350 nm and emission wavelength of 450–500 nm (Smith et al., 2004). Therefore, the synthesis of DPA during the sporulation in this study was monitored by three-dimensional fluorescence EEM spectrum, which is a powerful tool to distinguish vegetative cells from endospores (Liu et al., 2019). As shown in Fig. 4, two distinct peaks at E_x/E_m of 350/450 (peak A) and 450/550 nm (peak B) were appeared, which can be assigned to spores (DPA complex) and vegetative cells, respectively. The relative intensity of peak A/peak B in control and light alone experiments did not change very much within 48 h, while it was increased in NS alone and NS/light combined treatments, suggesting the NS mineral really can promote the intracellular synthesis of DPA complex. Specifically, the relative intensity of peak A/peak B at 48 h was obtained as 1.08, 1.04, 1.31 and 1.25 for the control, light alone, NS alone and NS/light combined system, respectively. Obviously, the relative intensity in NS/light combined system was lower than that of NS alone system, which indicates although NS alone could promote the DPA synthesis, the photocatalytic effect of NS mineral with light irradiation could suppress DPA synthesis and inhibit bacterial sporulation.

The release of DPA was further studied by measuring fluorescence emission of DPA-Tb^{3+} complex after adding Tb^{3+} in the filtrate samples.

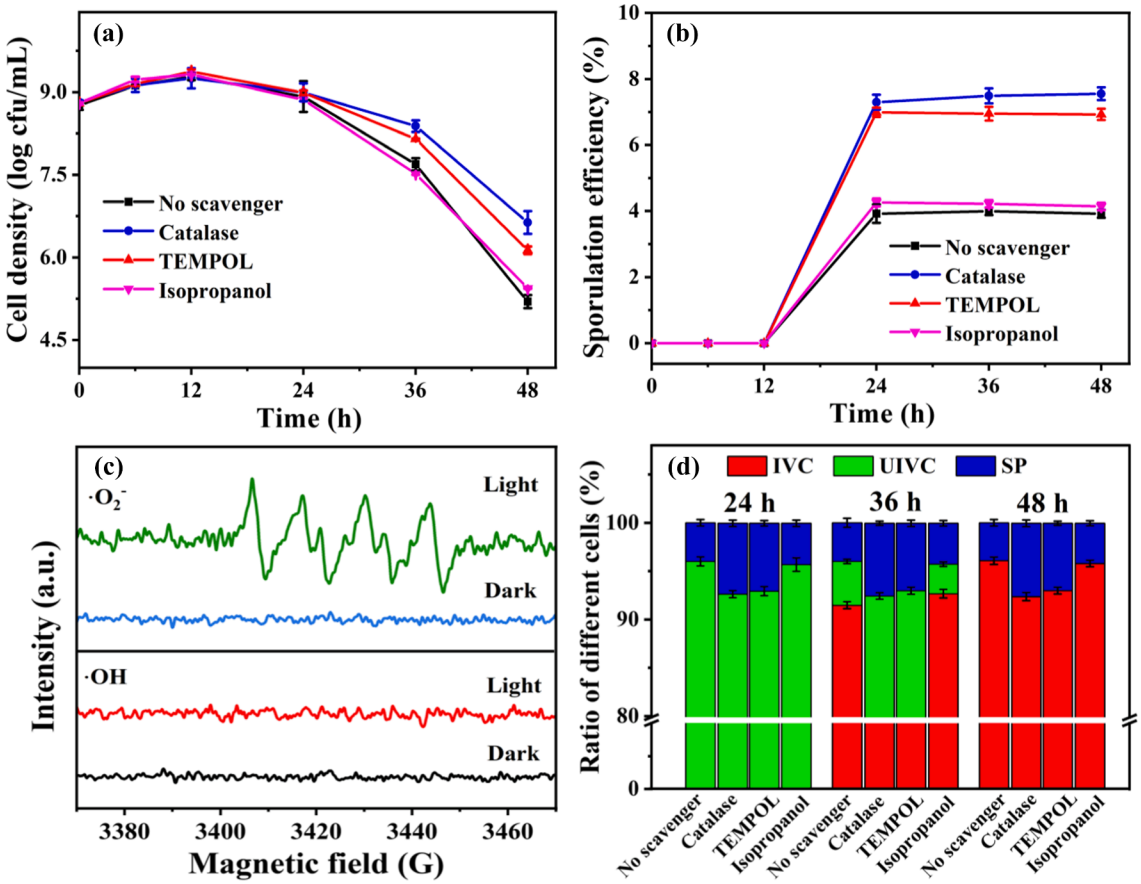

Fig. 3. (a) Changes of viable cell density, (b) sporulation efficiency with the addition of different scavengers; (c) Electron paramagnetic resonance (EPR) spectra for detecting $^{\cdot}O_2^-$ and $^{\cdot}OH$ either in dark or after light irradiation for 15 min; (d) Ratios of different statues of *B. subtilis* in NS/light system with the addition of different scavengers. (IVC: inactivated vegetative cells; UIVC: un-inactivated vegetative cells; SP: produced spores). Experimental condition: [Cell] = 1.0×10^9 cfu/mL, [NS] = 0.1 g/L, $[pH]_0$ = 8.5, [Isopropanol] = 0.5 mmol/L, [Catalase] = 300 U/mL, [TEMPOL] = 2 mmol/L.

To investigate the real-time changes of DPA release in the systems with and without light irradiation, the experiments were conducted in 24 h dark incubation, followed by 24 h light treatment. As shown in Fig. 5, no DPA was released with NS mineral under dark condition, while large amounts of DPA were released with NS and light combined system. DPA release is closely related to spore germination, and high rates of DPA release indicate high rates of spore death (Baloh and Sorg, 2022). This result suggests light treatment could stimulate spore germination. Moreover, the released DPA concentration in NS/light combined system was 2.19 times higher than that of light alone system (Fig. 5), suggesting the photocatalytic effect of NS interface could further accelerate the spore germination and spore death.

3.3.2. *Cell morphology changes and membrane damages*

To understand the bacterial sporulation process, the cell morphology changes at different systems in control, light alone, NS alone, and NS/light combined system were compared by SEM observations. As shown in Fig. 6, at initial time (0 h), almost all *B. subtilis* cells were in vegetative forms which exhibited plump long-rod shape. In control system, the cell morphology did not change very much with extended time to 48 h. While in light alone system, few of the cells began to swell, suggesting that light treatment leads to slight inactivation of vegetative cells, in agreement with Fig. 2a. In the case of NS alone, the long-rod shape of vegetative cells became short with fore-spore formed in the cells at 12 h. Finally, almost all the vegetative cells were transformed into globular endospores at 48 h. The cell morphology evolution in the NS/light combined system was similar to that of NS alone system, except that more cell debris and aggregates were found in the NS/light combined system, suggesting that photocatalytic effect of NS mineral leads to more inactivation and destruction of vegetative cells and decrease the absolute number of spores formed. This was further confirmed by using Wirtz-Conklin stain to distinguish vegetative cells from formed spores (Fig. S10). It was found that the number of spores (stained with green) at 48 h in NS/light combined system was lower than that of NS alone system due to the enhancement of ROSs produced from NS/light system.

The cell membrane integrity was investigated by SYTO 9/PI fluorescence assay according to (Olszewska et al., 2019). SYTO 9 is a green fluorescent membrane penetrant dye, which is used to stain nucleic acid in live bacteria with intact membrane, while PI can only enter cells with damaged membrane, quenching SYTO 9 emission and producing red fluorescence (Al-Hashimi et al., 2015). Results showed that the cells in light alone system exhibited green color within 48 h, which is similar to control experiments (Fig. S11). In contrast, a large portion of the cells in NS system became red at 48 h, suggesting the cell membrane was severely damaged due to the bactericidal effect of Zn^{2+} in the NS mineral. In addition, almost all the cells became red in the NS/light combined system, due to the enhanced ROSs generation by the photocatalytic effect. The change law was in accordance with bacterial inactivation efficiency, suggesting the bacterial inactivation and sporulation process at the NS mineral interfaces was closely associated with cell membrane damage.

3.3.3. *Physiological responses during sporulation*

To further understand the sporulation mechanisms, several intracellular physiological characteristics of *B. subtilis* vegetative cells and produced spores were comparably studied. Total protein was measured

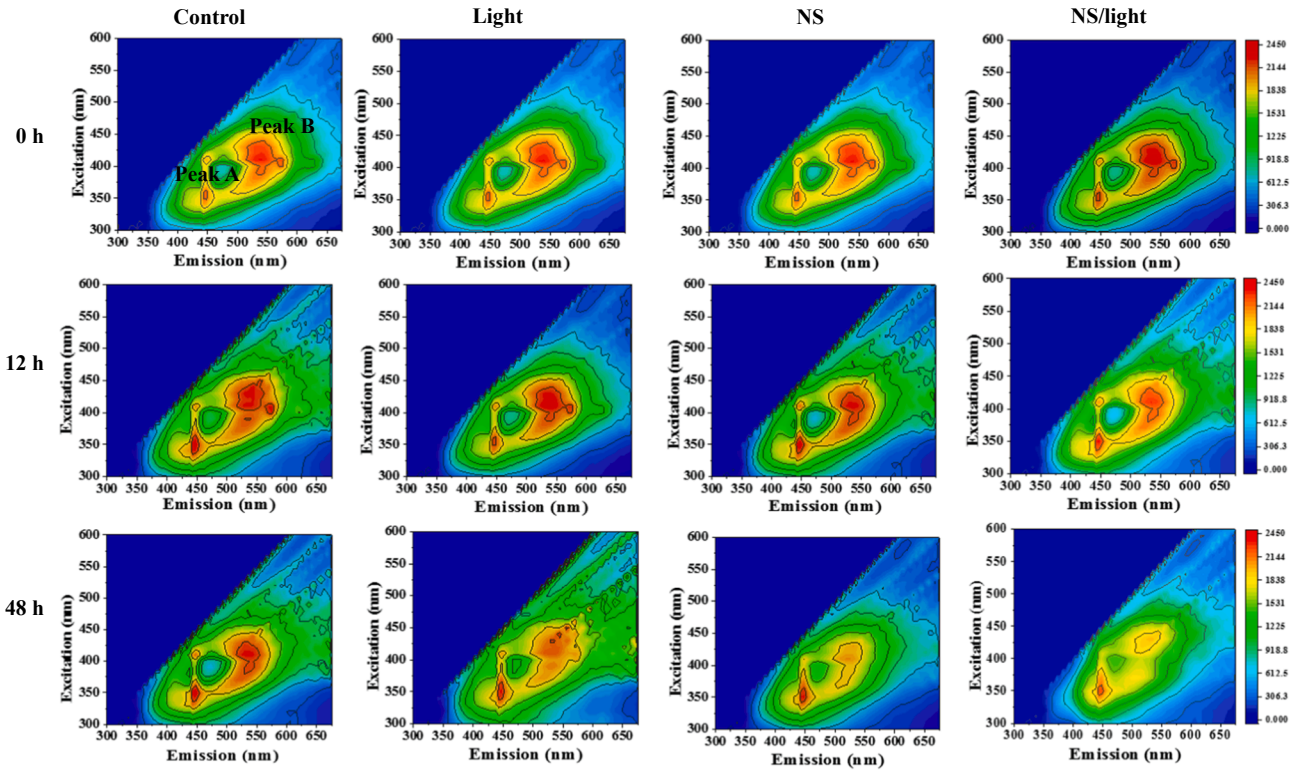

Fig. 4. Three-dimensional fluorescence Excitation-Emission-Matrix (EEM) spectrum of *B. subtilis* under control, light irradiation, NS alone and NS/light combined systems. Experimental condition: [Cell] = 1.0×10^9 cfu/mL, [NS] = 0.1 g/L, $[pH]_0$ = 8.5.

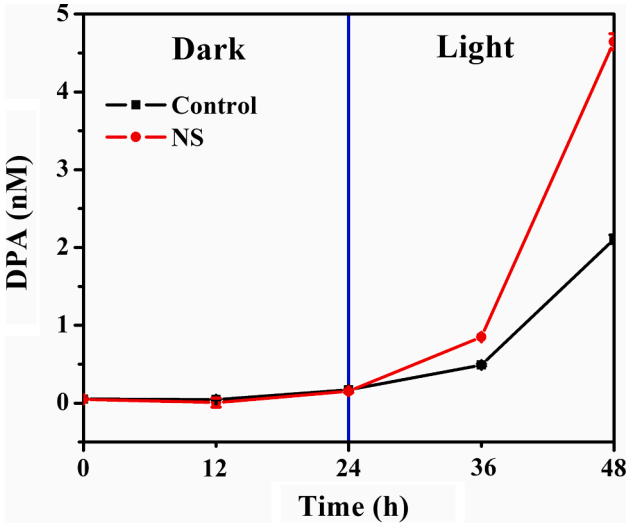

Fig. 5. Variation of released DPA concentration by *B. subtilis* cultured with NS for 12 h in dark condition, followed by 12 h light irradiation. Experimental condition: [Cell] = 1.0×10^9 cfu/mL, [NS] = 0.1 g/L, $[pH]_0$ = 8.5.

as a preliminary physiological factor to evaluate the cell metabolism activity according to previous literature (Wang et al., 2021, Zhang et al., 2013). In the control experiments, the total protein of vegetative cells did not change very much with extended cultivation time, while in the NS alone and NS/light combined system, the total protein was increased in the first 12 h and then decreased thereafter (Fig. 7a). This indicated that the oxidative stress accelerated the bacterial metabolism activity to produce more protein and supply more antioxidant enzymes at the initial stage. The NS/light combined system produced more protein than that of NS alone system, suggesting the ROSs generated by photocatalytic effect led to stronger physiological stress responses. The total proteins were all began to drop after 12 h, due to the inactivation of vegetative cells. However, the protein of produced spores was increased during the cultivation time to 48 h (Fig. S12a), which was obviously attributed to the continuous generation of spores and these results were in agreement with the sporulation efficiency in Fig. 2b.

The intracellular ROSs was then also monitored by using DCFH-DA probe according to the reported method (An et al., 2002, Wang et al., 2019). As shown in Fig. 7b, the intracellular ROSs level in light, NS alone and NS/light combined systems exhibited the trend of increase at the first 12 h followed by decrease up to 48 h. The maximal intracellular ROSs level at 12 h followed the order of NS/light combined system > NS alone > light alone, which indicates the external ROSs from photocatalysis also lead to high level of intracellular ROSs, resulting in faster and stronger oxidative stress. To further confirm the stress response in the bacterial sporulation process, the activity of antioxidant enzyme CAT (catalyze the decomposition of H_2O_2) was also monitored. Results showed that the NS/light combined system induced higher level of CAT than that of NS alone system (Fig. 7c), which was also consistent with the results of intracellular ROSs level, suggesting the photocatalytic effect of NS within light caused higher level of oxidative stress response in *B. subtilis* cells during sporulation.

Meanwhile, since the synthesis of ATP as energy storing matter in microbial cells was directly related to cellular metabolic activity (Dehghani et al., 2018), the ATP synthesis enzyme (ATPase) activity was also monitored to further clarify the variation of metabolism activity. It was found that the ATP content was increased in the initial 6 h of cultivation, and then decreased thereafter. Compared with the control and light alone systems, the ATP of cells in NS alone system was deceased more significantly, indicating the cell metabolic activity was inhibited by the NS mineral (Fig. 7d). The NS/light combined system could further decrease the ATP, suggesting the metabolism activity was severely damaged by the photocatalytic effect, leading to enhanced bacterial inactivation and reduced sporulation. In contrast, almost no ATP was

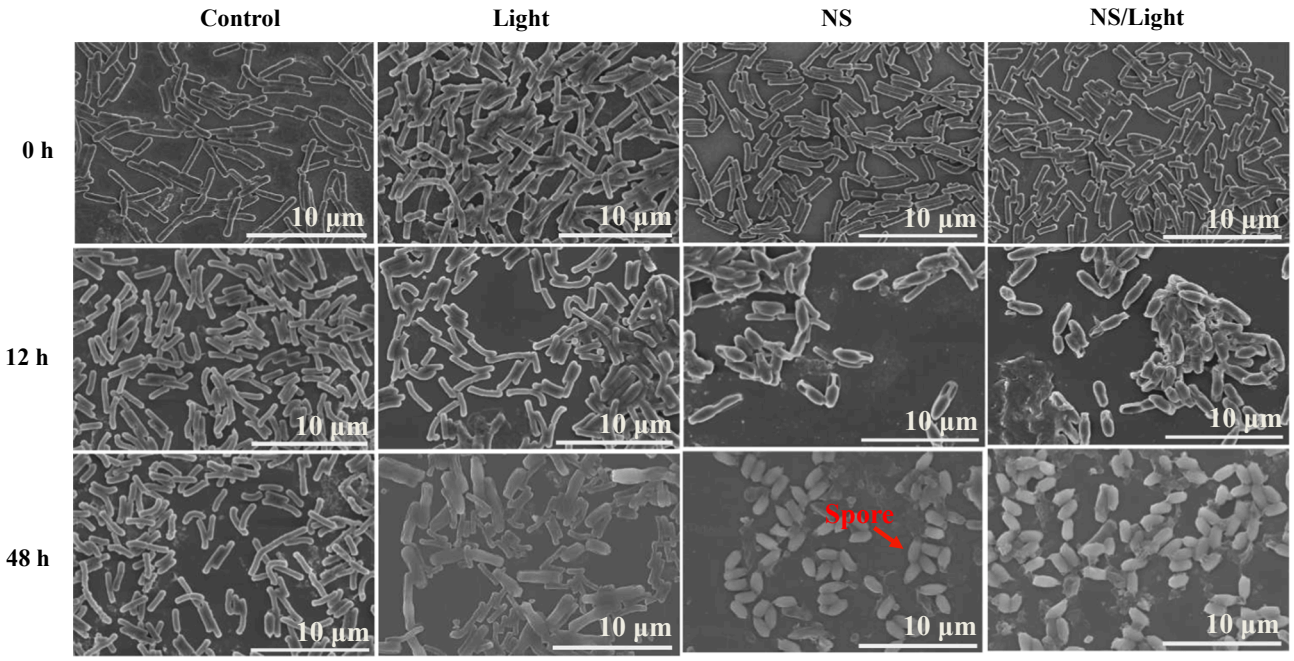

Fig. 6. Scanning electron microscopy (SEM) images of *B. subtilis* cells under control, light alone, NS alone and NS/light combined systems. Experimental condition: [Cell] = 1.0×10^9 cfu/mL, [NS] = 0.1 g/L, $[pH]_0$ = 8.5.

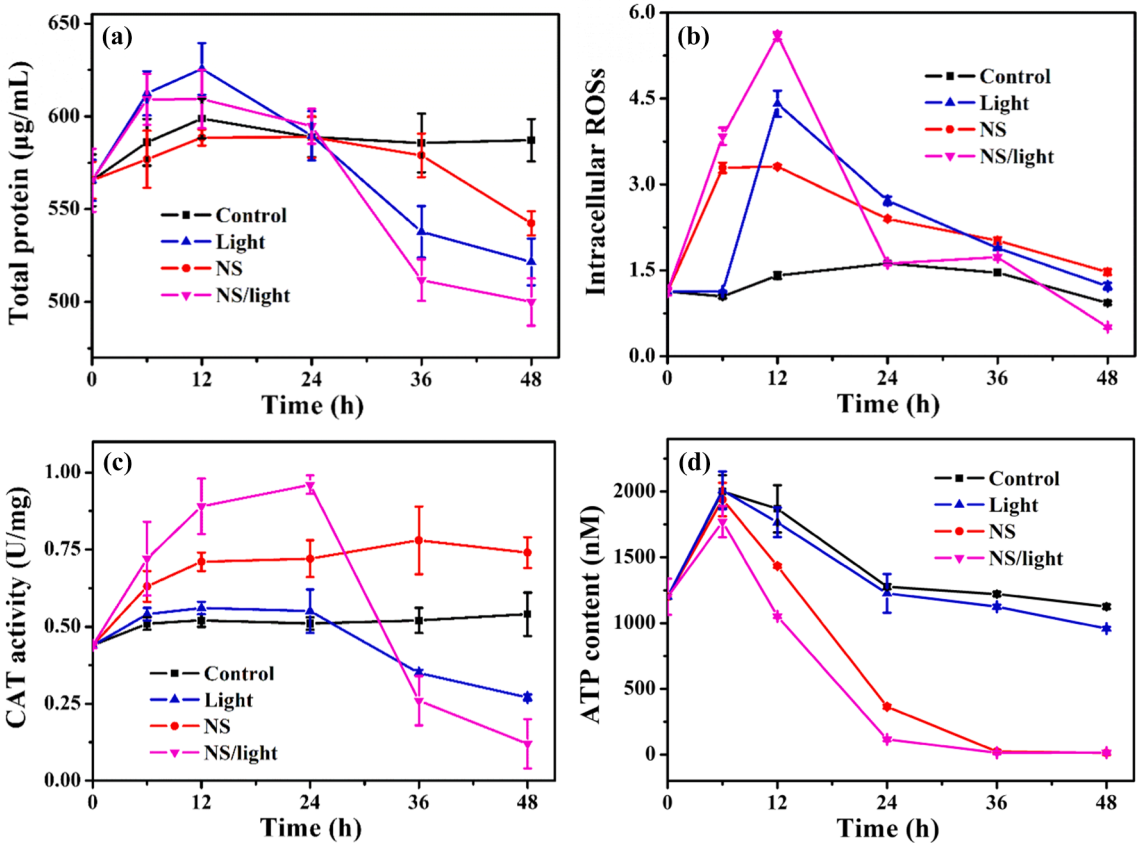

Fig. 7. Changes of (a) total protein content, (b) intracellular ROSs level, (c) catalase (CAT) activity and (d) ATP content during cultivation of *B. subtilis* under control, light irradiation, NS alone and NS/light combined treatment for 48 h. Experimental condition: [Cell] = 1.0×10^9 cfu/mL, [NS] = 0.1 g/L, $[pH]_0$ = 8.5.

detected in produced spores, suggesting the metabolic activity of produced spores was minimized and their physiological responses were insensitive to external oxidative stress (Fig. S12b). These results indicated that the photocatalytic effect of NS/light also led to the increased antioxidant enzyme activity and reduced ATP, which contributed to the suppression of bacterial sporulation.

Based on the above results, the interactions between *B. subtilis* and NS mineral with and without light irradiation was illustrated in Fig. 8. Under dark conditions, vegetative cells of *B. subtilis* were inactivated by released Zn^{2+} from NS, leading to the membrane damage and lethal effect to cause cell death, which was simultaneously accompanied by sub-lethal effect that involved the conversion of un-inactivated cells to spores to relief the adverse environment (Fig. 8a). In this sporulation process, DPA was synthesized and stored in the core of the formed spores, which was regulated by antioxidant enzyme systems. Under light irradiation system, the NS was excited with light irradiation to produce ROSs, in which H_2O_2 and $^{\bullet}O_2^-$ were the major reactive species to promote the bacterial inactivation and inhibit bacterial sporulation. The sporulation efficiency decreased from 8.1 % to 4.5 %. Antioxidant enzyme activity was increased, and higher level of defending system was induced, followed by the reduced ATP and release of DPA, which significantly inhibit the bacterial sporulation process (Fig. 8b). In addition, no changes of XRD peaks of NS before and after the reaction were found (Fig. S13), suggesting the NS mineral had substantial photostability and durability. Previous studies have investigated the effects of various environmental factors such as temperature, pH and water activity (Gauvry et al., 2021), as well as metal ions (Sinnelä et al., 2019) and nutrient components (Posada-Uribe et al., 2015) on the *B. subtilis* sporulation efficiencies. It was found that nutrient deficiency and some of metal ions (Ca^{2+}, Mn^{2+}) could stimulate the bacterial sporulation. However, no studies have investigated the effect of natural minerals on the sporulation efficiency and mechanisms. We found that NS could also stimulate the *B. subtilis* sporulation under dark condition, while the sporulation efficiency could be significantly inhibited under light irradiation due to the photocatalytic effect.

To better understand the interactions between natural minerals and spore-producing bacteria under long-term exposure to natural water environment. The cultivation experiments were extended to 9 days (216 h), and the overall tendency of the result was found to be similar to above 48 h experiments with inactivation efficiency following the order of NS/light combined system > NS alone > light, and sporulation efficiency following the order of NS alone > NS/light combined system > light (Fig. S14). A relative high sporulation efficiency was found in negative control due to the depletion of nutrients. These results doubly confirmed that the photocatalytic effect of NS/light could enhance bacterial inactivation while prevent undesired spore formation to some extent, which can be used in designing suitable protocols for spore-contaminated water disinfection. Moreover, the NS mineral used in the disinfection process was naturally occurring mineral which can be obtained in large quantity without artificial chemical synthesis. The estimated market price of NS mineral was only ¥ ~10/kg, and the energy input could be inexhaustible sunlight. Therefore, the proposed disinfection method was cost-effective and had potential for large-scale applications.

4. Conclusions

In summary, the interacting mechanisms between natural minerals and spore-producing bacteria were comparably explored with and without light irradiation for the first time, using NS and *B. subtilis* as typical natural mineral and typical bacteria examples. It was found that NS could inactivate vegetative cells of *B. subtilis* and promote the vegetative cells to produce spores under dark condition. The released Zn^{2+} from NS was mainly responsible for the bacterial inactivation and

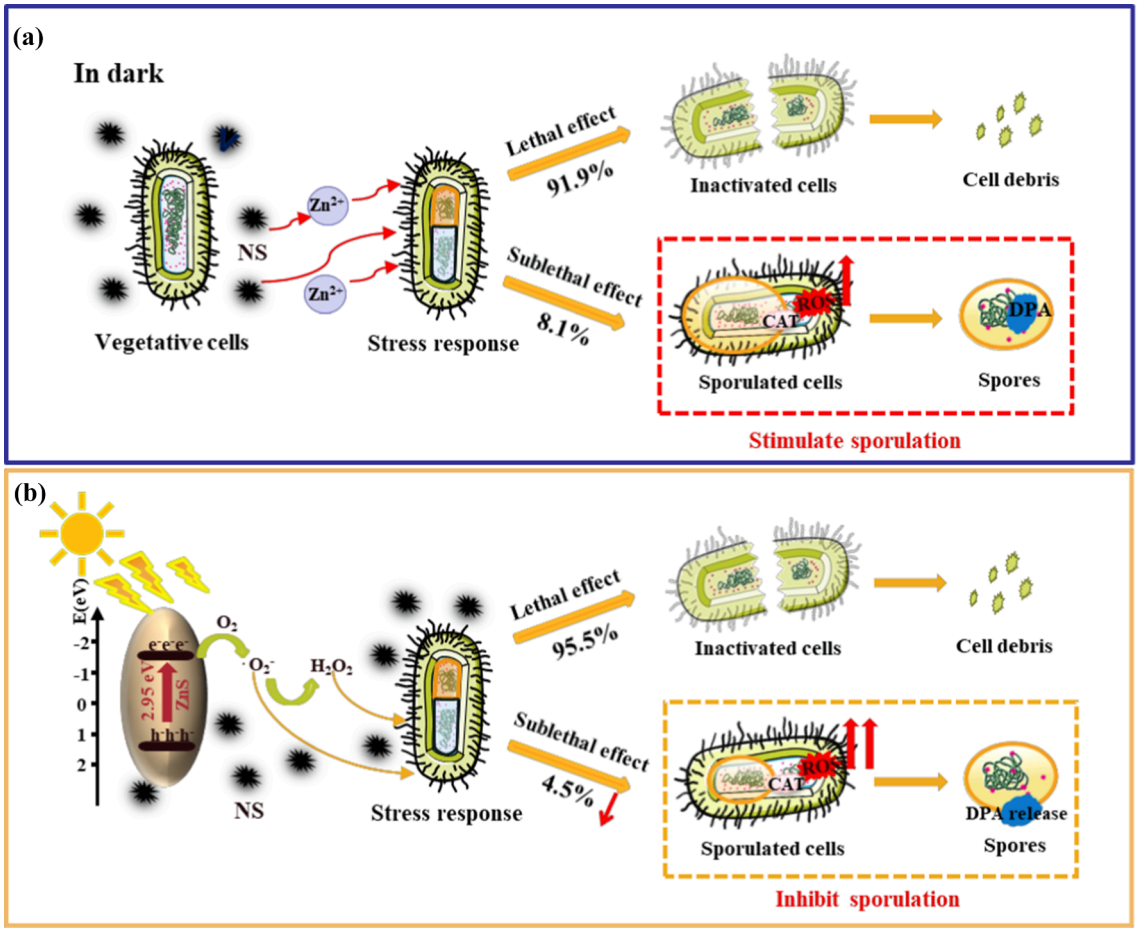

Fig. 8. Schematic illustrating the bacterial sporulation mechanisms of *B. subtilis* at NS interface under (a) dark condition and (b) light irradiation.

sporulation. With light irradiation, the inactivation efficiency of *B. subtilis* by NS/light combined system was increased, while the sporulation efficiency was decreased from 8.1 % to 4.5 %, because more vegetative cells were killed before they could transform to spores to relief oxidative stress. The sub-lethal effect was weakened, leading to increased bacterial inactivation efficiency. The H_2O_2 and $^{\bullet}O_2^-$ were found to be major reactive species for the bacterial inactivation and suppression of bacterial sporulation in this simulation of natural photocatalytic system. The presence of NS could promote the DPA synthesis under dark, however, the photocatalytic effect of NS/light combined system led to the release of DPA and suppress the DPA synthesis. SEM observation visually confirmed the transformation process from vegetative cells to spores. Mechanistic study further indicated the bacterial sporulation was associated with physiological responses including the damage of cell membrane integrity, induction of anti-oxidant enzyme activity and ATP reduce. Similar phenomenon was also found with long-term photocatalytic treatment up to 9 d, further confirming the photocatalytic effect could promote the inactivation of spore-producing bacteria while inhibit their sporulation.

These results not only provide in-depth understanding of the interactions between natural minerals and spore-producing bacteria, but also reveal the mechanistic linkage between sub-lethal stress responses and bacterial sporulation. Moreover, in water disinfection fields, the inactivation of spore-producing bacteria is often accompanied with their sporulation. Once spores are formed, it is difficult to be further inactivated, imposing more threats to human health. The study also highlights the possibility of developing photocatalysis-based protocols to prevent bacterial sporulation, thus these kinds of bacteria can be inactivated before transformed into the spores during water disinfection.

CRediT authorship contribution statement

Wanjun Wang: Formal analysis, Methodology, Writing – original draft. **Yan Liu:** Formal analysis, Methodology. **Guiying Li:** Investigation. **Zhenni Liu:** Investigation. **Po Keung Wong:** Validation. **Taicheng An:** Conceptualization, Supervision.

Declaration of Competing Interest

The authors declare that they have no known competing financial interests or personal relationships that could have appeared to influence the work reported in this paper.

Data availability

No data was used for the research described in the article.

Acknowledgements

This work was supported by the National Natural Science Foundation of China (42122056, U1901210, and 42077333), National Key Research and Development Program of China (2019YFC1804501), Guangdong Basic and Applied Basic Research Foundation (2021B1515020063), Science and Technology Program of Guangzhou, China (202002030177), Key Research and Development Program of Guangdong Province (2021B1111380003), and Local Innovative and Research Teams Project of Guangdong Pearl River Talents Program (2017BT01Z032).

Appendix A. Supplementary material

Supplementary data to this article can be found online at https://doi.org/10.1016/j.envint.2022.107460.

References

Al-Hashimi, A.M., Mason, T.J., Joyce, E.M., 2015. Combined effect of ultrasound and ozone on bacteria in water. Environ. Sci. Technol. 49 (19), 11697–11702.
An, T.C., Zhu, X.H., Xiong, Y., 2002. Feasibility study of photoelectrochemical degradation of methylene blue with three-dimensional electrode-photocatalytic reactor. Chemosphere 46 (6), 897–903.
Aubineau, J., El Albani, A., Bekker, A., Somogyi, A., Bankole, O.M., Macchiarelli, R., Meunier, A., Riboulleau, A., Reynaud, J.Y., Konhauser, K.O., 2019. Microbially induced potassium enrichment in Paleoproterozoic shales and implications for reverse weathering on early Earth. Nat. Commun. 10 (1), 1–9.
Baloh, M., Sorg, J.A., 2022. Clostridioides difficile spore germination: initiation to DPA release. Curr. Opin. Microbiol. 65, 101–107.
Berberidou, C., Paspaltsis, I., Pavlidou, E., Sklaviadis, T., Poulios, I., 2012. Heterogenous photocatalytic inactivation of B. stearothermophilus endospores in aqueous suspensions under artificial and solar irradiation. Appl. Catal. B: Environ. 125, 375–382.
Cai, Y., Liu, J., Li, G., Wong, P.K., An, T., 2021. Formation mechanisms of viable but nonculturable bacteria through induction by light-based disinfection and their antibiotic resistance gene transfer risk: A review. Crit. Rev. Environ. Sci. Technol. https://doi.org/10.1080/10643389.10642021.11932397.
Chen, M., Cai, Y.W., Li, G.Y., Zhao, H.J., An, T.C., 2022. The stress response mechanisms of biofilm formation under sub-lethal photocatalysis. Appl. Catal. B: Environ. 307, 121200.
Chen, R., Li, J., Wang, H., Chen, P., Dong, X.a., Sun, Y., Zhou, Y., Dong, F., 2021. Photocatalytic reaction mechanisms at the gas-solid interface for typical air pollutants decomposition. J. Mater. Chem. A 9(36), 20184-20210.
Chen, Y.M., Lu, A.H., Li, Y., Zhang, L.Z., Yip, H.Y., Zhao, H.J., An, T.C., Wong, P.K., 2011. Naturally occurring sphalerite as a novel cost-effective photocatalyst for bacterial disinfection under visible light. Environ. Sci. Technol. 45 (13), 5689–5695.
Chen, X.F., Yin, H.L., Li, G.Y., Wang, W.J., Wong, P.K., Zhao, H.J., An, T.C., 2019. Antibiotic-resistance gene transfer in antibiotic-resistance bacteria under different light irradiation: Implications from oxidative stress and gene expression. Water Res. 149, 282–291.
Cuadros, J., 2017. Clay minerals interaction with microorganisms: a review. Clay Miner. 52 (2), 235–261.
De Sordi, L., Butt, M.A., Pye, H., Kohoutova, D., Mosse, C.A., Yahioglu, G., Stamati, I., Deonarain, M., Battah, S., Ready, D., 2015. Development of photodynamic antimicrobial chemotherapy (PACT) for Clostridium difficile. PLoS One 10 (8), e0135039.
Dehghani, S., Rezaee, A., Hosseinkhani, S., 2018. Effect of alternating electrical current on denitrifying bacteria in a microbial electrochemical system: biofilm viability and ATP assessment. Environ. Sci. Pollut. Res. 25 (33), 33591–33598.
Fan, L., Hou, F., Muhammad, A.I., Ruiling, L., Watharkar, R.B., Guo, M., Ding, T., Liu, D., 2019. Synergistic inactivation and mechanism of thermal and ultrasound treatments against *Bacillus subtilis* spores. Food Res. Int. 116, 1094–1102.
Gauvry, E., Mathot, A.G., Couvert, O., Leguerinel, I., Coroller, L., 2021. Effects of temperature, pH and water activity on the growth and the sporulation abilities of Bacillus subtilis BSB1. Int. J. Food Microbiol. 337, 108915.
Geeraerd, A.H., Valdramidis, V., Van Impe, J.F., 2005. GInaFiT, a freeware tool to assess non-log-linear microbial survivor curves. Int. J. Food Microbiol. 102 (1), 95–105.
González-Tortuero, E., Rodríguez-Beltrán, J., Radek, R., Blázquez, J., Rodríguez-Rojas, A., 2018. Clay-induced DNA breaks as a path for genetic diversity, antibiotic resistance, and asbestos carcinogenesis. Sci. Rep. 8 (1), 1–10.
Hamouda, T., Shih, A., Baker, J., 2002. A rapid staining technique for the detection of the initiation of germination of bacterial spores. Lett. Appl. Microbiol. 34 (2), 86–90.
Kort, R., O'brien, A.C., Van Stokkum, I.H., Oomes, S.J., Crielaard, W., Hellingwerf, K.J., Brul, S., 2005. Assessment of heat resistance of bacterial spores from food product isolates by fluorescence monitoring of dipicolinic acid release. Appl. Environ. Microbiol. 71 (7), 3556–3564.
Li, G.Y., Nie, X., Chen, J.Y., Jiang, Q., An, T.C., Wong, P.K., Zhang, H.M., Zhao, H.J., Yamashita, H., 2015. Enhanced visible-light-driven photocatalytic inactivation of *Escherichia coli* using g-C_3N_4/TiO_2 hybrid photocatalyst synthesized using a hydrothermal-calcination approach. Water Res. 86, 17–24.
Li, G.Y., Chen, X.F., Yin, H.L., Wang, W.J., Wong, P.K., An, T.C., 2020. Natural sphalerite nanoparticles can accelerate horizontal transfer of plasmid-mediated antibiotic-resistance genes. Environ. Int. 136, 105497.
Li, Y., Li, X., Wang, D., Shen, C., Yang, M., 2018b. Hydroxyapatite nanoparticle based fluorometric turn-on determination of dipicolinic acid, a biomarker of bacterial spores. Microchim. Acta 185 (9), 1–5.
Li, Q., Yang, J., Fan, W., Zhou, D., Wang, X., Zhang, L., Huo, M., Crittenden, J.C., 2018a. Different transport behaviors of Bacillus subtilis cells and spores in saturated porous media: implications for contamination risks associated with bacterial sporulation in aquifer. Colloids Surf. B 162, 35–42.
Li, K., Zhao, X., Hammer, K., B., Du, S., Chen, Y., 2013. Nanoparticles inhibit DNA replication by binding to DNA: modeling and experimental validation. ACS Nano 7 (11), 9664–9674.
Liu, M.L., Chen, B.B., He, J.H., Li, C.M., Li, Y.F., Huang, C.Z., 2019. Anthrax biomarker: An ultrasensitive fluorescent ratiometry of dipicolinic acid by using terbium (III)-modified carbon dots. Talanta 191, 443–448.
Liu, C., Mao, S., Shi, M., Wang, F., Xia, M., Chen, Q., Ju, X., 2021. Peroxymonosulfate activation through 2D/2D Z-scheme CoAl-LDH/BiOBr photocatalyst under visible light for ciprofloxacin degradation. J. Hazard. Mater. 420, 126613.
Liu, C., Mao, S., Wang, H., Wu, Y., Wang, F., Xia, M., Chen, Q., 2022. Peroxymonosulfate-assisted for facilitating photocatalytic degradation performance of 2D/2D WO_3/BiOBr S-scheme heterojunction. Chem. Eng. J. 430, 132806.

Lu, A., Li, Y., Jin, S., Wang, X., Wu, X.-L., Zeng, C., Ding, H., Hao, R., Lv, M., Wang, C., 2012. Growth of non-phototrophic microorganisms using solar energy through mineral photocatalysis. Nat. Commun. 3 (1), 1–8.
McMahon, S., Anderson, R.P., Saupe, E.E., Briggs, D.E., 2016. Experimental evidence that clay inhibits bacterial decomposers: implications for preservation of organic fossils. Geology 44 (10), 867–870.
Mohammadi, S., Moussavi, G., Shekoohiyan, S., Marín, M.L., Boscá, F., Giannakis, S., 2021. A continuous-flow catalytic process with natural hematite-alginate beads for effective water decontamination and disinfection: Peroxymonosulfate activation leading to dominant sulfate radical and minor non-radical pathways. Chem. Eng. J. 411, 127738.
Moradi, M., Kalantary, R.R., Esrafili, A., Jafari, A.J., Gholami, M., 2017. Visible light photocatalytic inactivation of *Escherichia coli* by natural pyrite assisted by oxalate at neutral pH. J. Mol. Liq. 248, 880–889.
Mtimet, N., Trunet, C., Mathot, A.-G., Venaille, L., Leguérinel, I., Coroller, L., Couvert, O., 2015. Modeling the behavior of *Geobacillus stearothermophilus* ATCC 12980 throughout its life cycle as vegetative cells or spores using growth boundaries. Food Microbiol. 48, 153–162.
Mueller, B., 2015. Experimental interactions between clay minerals and bacteria: a review. Pedosphere 25 (6), 799–810.
Nishikawa, M., Kobayashi, K., 2021. Calcium prevents biofilm dispersion in *Bacillus subtilis*. J. Bacteriol. 203 (14), e00114–e001121.
Olszewska, M.A., Nynca, A., Białobrzewski, I., Kocot, A.M., Łaguna, J., 2019. Assessment of the bacterial viability of chlorine-and quaternary ammonium compounds-treated Lactobacillus cells via a multi-method approach. J. Appl. Microbiol. 126 (4), 1070–1080.
Pandey, R., Ter Beek, A., Vischer, N.O., Smelt, J.P., Brul, S., Manders, E.M., 2013. Live cell imaging of germination and outgrowth of individual *Bacillus subtilis* spores; the effect of heat stress quantitatively analyzed with SporeTracker. PLoS One 8 (3), e58972.
Peng, X., Ng, T.W., Huang, G., Wang, W., An, T., Wong, P.K., 2017. Bacterial disinfection in a sunlight/visible-light-driven photocatalytic reactor by recyclable natural magnetic sphalerite. Chemosphere 166, 521–527.
Posada-Uribe, L.F., Romero-Tabarez, M., Villegas-Escobar, V., 2015. Effect of medium components and culture conditions in *Bacillus subtilis* EA-CB0575 spore production. Bioproc. Biosyst. Eng. 38 (10), 1879–1888.
Qi, Z.L., Li, G.Y., Wang, M., Chen, C.L., Xu, Z., An, T.C., 2022. Photoelectrocatalytic inactivation mechanism of *E. coli* DH5α (TET) and synergistic degradation of corresponding antibiotics in water. Water Res. 215, 118240.
Redan, B.W., Morrissey, T.R., Rolfe, C.A., Aguilar, V.L., Skinner, G.E., Reddy, N.R., 2022. Rapid detection and quantitation of dipicolinic acid from *Clostridium botulinum* spores using mixed-mode liquid chromatography-tandem mass spectrometry. Anal. Bioanal. Chem. 414 (8), 2767–2774.
Sella, S.R., Vandenberghe, L.P., Soccol, C.R., 2014. Life cycle and spore resistance of spore-forming *Bacillus atrophaeus*. Microbiol. Res. 169 (12), 931–939.
Sheng, J., Li, X., Xu, Y., 2014. Generation of H_2O_2 and OH radicals on Bi_2WO_6 for phenol degradation under visible light. ACS Catal. 4 (3), 732–737.
Singh, R., Edokpayi, J.N., Odiyo, J.O., Smith, J.A., 2019. *E. coli* inactivation by metals and effects of changes in water chemistry. J. Environ. Eng. 145 (2), 04018136.
Sinnelä, M.T., Park, Y.K., Lee, J.H., Jeong, K.C., Kim, Y.W., Hwang, H.J., Mah, J.H., 2019. Effects of calcium and manganese on sporulation of *Bacillus* species involved in food poisoning and spoilage. Foods 8 (4), 119.
Smith, C.B., Anderson, J.E., Webb, S.R., 2004. Detection of *Bacillus* endospores using total luminescence spectroscopy. Spectrochimica acta. Part A, Mol. Biomol. Spectrosc. 60 (11), 2517–2521.
Tehri, N., Kumar, N., Raghu, H.V., Vashishth, A., 2018. Biomarkers of bacterial spore germination. Ann. Microbiol. 68 (9), 513–523.
Tewari, A., Abdullah, S., 2015. *Bacillus cereus* food poisoning: international and Indian perspective. J. Food Sci. Technol. 52 (5), 2500–2511.
Wang, W.J., Li, G.Y., Xia, D.H., An, T.C., Zhao, H.J., Wong, P.K., 2017. Photocatalytic nanomaterials for solar-driven bacterial inactivation: recent progress and challenges. Environ. Sci.-Nano 4 (4), 782–799.
Wang, W.J., Wang, H.N., Li, G.Y., An, T.C., Zhao, H.J., Wong, P.K., 2019. Catalyst-free activation of persulfate by visible light for water disinfection: Efficiency and mechanisms. Water Res. 157, 106–118.
Wang, W.J., Wang, H.N., Li, G.Y., Wong, P.K., An, T.C., 2020. Visible light activation of persulfate by magnetic hydrochar for bacterial inactivation: Efficiency, recyclability and mechanisms. Water Res. 176, 115746.
Wang, W.J., Xie, H.J., Li, G.Y., Li, J., Wong, P.K., An, T.C., 2021. Visible light-induced marine bacterial inactivation in seawater by an in situ photo-Fenton system without additional oxidants: Implications for ballast water sterilization. ACS ES&T Water 1 (6), 1483–1494.
Wilson, L.A., Butterfield, N.J., 2014. Sediment effects on the preservation of Burgess Shale–type compression fossils. Palaios 29 (4), 145–154.
Xu, Y., Wang, C., Hou, J., Dai, S.S., Wang, P.F., Miao, L.Z., Lv, B.W., Yang, Y.Y., You, G. X., 2016. Effects of ZnO nanoparticles and Zn^{2+} on fluvial biofilms and the related toxicity mechanisms. Sci. Total Environ. 544, 230–237.
Yin, H.L., Chen, X.F., Li, G.Y., Wang, W.J., Wong, P.K., An, T.C., 2021. Can photocatalytic technology facilitate conjugative transfer of ARGs in bacteria at the interface of natural sphalerite under different light irradiation? Appl. Catal. B-Environ. 287, 119977.
Zhang, W., Hughes, J., Chen, Y., 2012. Impacts of hematite nanoparticle exposure on biomechanical, adhesive, and surface electrical properties of *Escherichia coli* cells. Appl. Environ. Microbiol. 78 (11), 3905–3915.
Zhang, L.S., Wong, K.H., Yip, H.Y., Hu, C., Yu, J.C., Chan, C.Y., Wong, P.K., 2010. Effective photocatalytic disinfection of *E. coli* K-12 using AgBr−Ag−Bi_2WO_6 nanojunction system irradiated by visible light: the role of diffusing hydroxyl radicals. Environ. Sci. Technol. 44 (4), 1392–1398.
Zhang, C., Yi, Y.L., Hao, K., Liu, G.L., Wang, G.X., 2013. Algicidal activity of Salvia miltiorrhiza Bung on *Microcystis aeruginosa*—Towards identification of algicidal substance and determination of inhibition mechanism. Chemosphere 93 (6), 997–1004.
Zhou, C.H., Zhao, L.Z., Wang, A.Q., Chen, T.H., He, H.P., 2016. Current fundamental and applied research into clay minerals in China. Appl. Clay Sci. 119, 3–7.